Linearity and frequency response of pneumotachographs

K. E. Finucane, B. A. Egan and S. V. Dawson

J Appl Physiol 32:121-126, 1972. ;

Journal of Applied Physiology publishes original papers that deal with diverse area of research in applied physiology, especially those papers emphasizing adaptive and integrative mechanisms. It is published 12 times a year (monthly) by the American Physiological Society, 9650 Rockville Pike, Bethesda MD 20814-3991. ISSN: 8750-7587, ESSN: 1522-1601. Visit our website at http://www.the-aps.org/.

JOURNAL OF APPLIED PHYSIOLOGY
Vol. 32, No. 1, January 1972. *Printed in U.S.A.*

SPECIAL COMMUNICATIONS

Linearity and frequency response of pneumotachographs

KEVIN E. FINUCANE, BRUCE A. EGAN, AND STANLEY V. DAWSON
Departments of Physiology and Environmental Health Sciences, Harvard School of Public Health, Boston, Massachusetts 02115

FINUCANE, KEVIN E., BRUCE A. EGAN, AND STANLEY V. DAWSON. *Linearity and frequency response of pneumotachographs.* J. Appl. Physiol. 32(1): 121–126. 1972.—Flow-pressure characteristics of commonly used capillary tube and screen flowmeters were obtained for steady state and periodic flows. *Steady flow:* pressure drop (ΔP) depended upon the geometry upstream from the flowmeter, was nonlinear in flow, and in the nominal linear range deviated from linearity by 7–14%. *Periodic flow:* because of the inertia of gas in capillary flowmeters, flow lagged ΔP, and its amplitude decreased relative to the steady flow at that ΔP. At 10 cycles/sec phase lag and amplitude decrease were 8° and 1% in air and 29° and 15% in sulfur hexafluoride. Accurate estimates of flow therefore require information of flow-pressure characteristics of flowmeters obtained in the range of flows and circumstances proposed for measurement. Upstream geometry influences the distribution of flow among the pathways of a flowmeter, ΔP being a function of both the distribution of flow and disturbances to flow associated with flowmeter geometry. Theoretical analysis of an idealized geometry related the distribution of steady flow to overall pressure drop, upstream velocity distribution, and flowmeter resistance.

measurement of flow; distribution of steady flow among parallel pathways of a resistive element

THIS PAPER DESCRIBES the steady-state flow-pressure ($\dot{V}$-P) characteristics and the frequency response of the two types of pneumotachograph, or gas flowmeter, in most common use: the type devised and introduced by Fleisch (1), in which the resistive element consists of many capillary tubes in parallel, and the type introduced by Silverman and Whittenberger (4), in which the resistive element is a 400-mesh wire screen. The study was stimulated by three observations which suggested that accurate measurements of flow were technically more difficult than we had previously appreciated. The observations were: *1*) at any steady flow rate the pressure drop across a Fleisch flowmeter (ΔPf) changed when the geometry of the tubing upstream from it was changed; *2*) during periodic flow, ΔPf and flow were out of phase; and *3*) the pressure drop across screen flowmeters (ΔPs) was a nonlinear function of flow rate even at low flow rates and when the area of the screen was relatively large (~60 cm²).

Fry et al. (2) evaluated the physical properties of three types of resistive element—concentric cylinders, 325-mesh screen, and parallel vertical plates. No detailed study of flowmeter behavior has been reported since then. The present study shows how upstream geometry influences the $\dot{V}$-P behavior of flowmeters and describes the effect of periodic flow on the phase and amplitude of pressure drop with respect to flow. The results define limitations of these flowmeters pertinent to the measurement of flow rate in the laboratory; they suggested that the steady-state $\dot{V}$-P behavior was determined in part by the distribution of flow among the parallel pathways of the flowmeter and that this in turn was a function both of the resistance of the flowmeter and of the distribution of velocity across the section of the pipe upstream from it. The relationships between resistance, mean velocity, and the upstream velocity distribution in determining the distribution of steady flow among the parallel pathways of a resistive element are analyzed in the APPENDIX. The analytical and empirical results provide information which may be useful in improving the design of flowmeters.

METHODS

Three sizes of Fleisch flowmeter (Instrumentation Associates, models 2, 3 and 4) and four screen flowmeters were examined; the largest screen had an area of 62 cm² and the smallest an area of 3.1 cm².

The steady-state $\dot{V}$-P behavior of a flowmeter was assessed by measuring the pressure drop across it during steady rates of flow produced by drawing gas at room temperature (20 C) through the flowmeter with a vacuum cleaner. Pressures were measured with differential pressure transducers (Sanborn, models 268B or 270) coupled to carrier preamplifiers (Hewlett-Packard model 200-1000) and the resulting signals recorded (Sanborn, model 300). The transducers had common-mode rejection ratios of 100% over the range of pressures and frequencies encountered. Flow was measured by observing the rate of displacement of the bell of a balanced 120-liter spirometer (Collins, model 793) connected in series with the flowmeter. The spirometer was the standard for all measurements of flow; when other flowmeters were used they were calibrated with this standard and then used without changing the geometry of the immediately adjacent conducting tubing. An orifice meter and a no. 4 Fleisch flowmeter, which was preceded by a 20-cm-long pipe with the same internal diameter as the flowmeter and by a cone with walls which diverged at about 15° from the axis of flow, were the alternative means used for estimating flow rate. The drag coefficient[1] (C_D) of the orifice meter was 12.26 and was independent of flow rate for flows <14 liters/sec. The ΔPf of the Fleisch flowmeter was linear in flow from 0 to 7.5 liters/sec.

To assess the influence of upstream geometry on the $\dot{V}$-P behavior of flowmeters we made systematic changes in the diameter, length, and convergence or divergence from the axis of flow of the pipes immediately upstream from the flowmeter; details of some of the geometries used are shown in Fig. 1. In these experiments the mean flow rate through the small flowmeters was estimated with the no. 4 flowmeter (see above), situated approximately 150 cm upstream from the flowmeter being examined; flow rate through the large flowmeters was estimated with the orifice meter situated downstream from the flowmeter being examined.

[1] $C_D = 2 \cdot \text{area} \cdot \text{pressure/density} \cdot \text{flow rate}$.

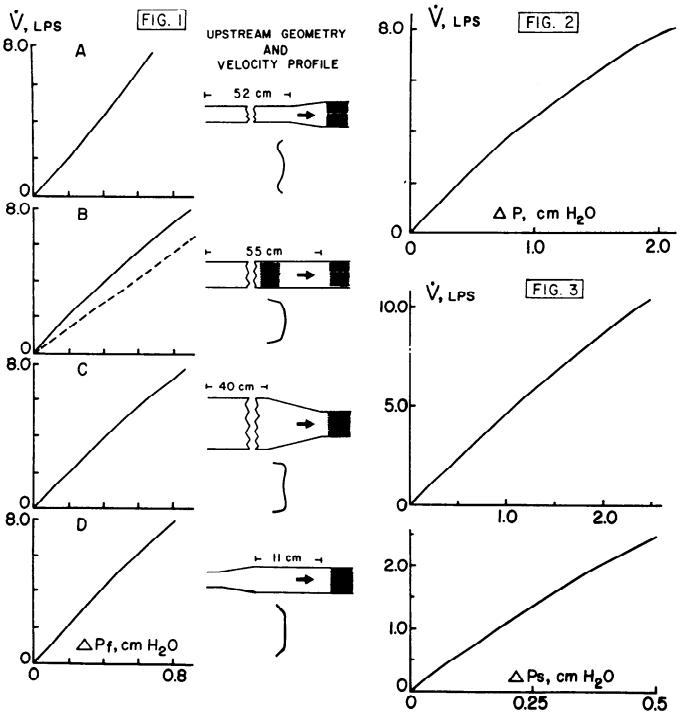

FIG. 1. V̇-P curves of no. 3 Fleisch flowmeter with upstream geometry and probable velocity profile pertinent to each measurement; interrupted line represents predicted V̇-P relationship.

FIG. 2. Relationship between flow and total ΔPf of no. 3 Fleisch flowmeter.

FIG. 3. V̇-P curves of a 62-cm² 400-mesh screen (*top*) and of a 12.6-cm² screen (*bottom*).

Absolute pressure, and therefore gas density, in the test flowmeters varied little during a V̇-P measurement (<6 cm H_2O) and from one geometry to another; room temperature was virtually constant.

The V̇-P characteristics of Fleisch and screen flowmeters were also examined in circumstances which would pertain to their use as the resistive elements in "flow" plethysmographs.[2] The flowmeter, with no conducting tubing upstream or downstream from it, was placed in a hole in the wall of a 200-liter chamber. The total pressure drop across the flowmeter[3] was measured as the pressure difference between the atmosphere and the pressure inside the chamber measured at a distance from the flowmeter. Air was drawn from the room directly through the flowmeter into the chamber and flow was measured with an orifice meter situated between the chamber and the pump.

Frequency Response

The frequency response was assessed over the range of frequencies 1–10 cycles/sec on both air and sulfur hexafluoride (SF_6). The standard for phase distortion was the output of an accelerometer; amplitude distortion was assessed by comparing the amplitude of the pressure drop across the flowmeter at each frequency with the amplitude of flow.

The accelerometer was constructed in the laboratory and consisted of a linear displacement transducer (Schaevitz, 020 x-c), the core of which was mounted on the end of a phosphor bronze strip 36 x 5.8 x 0.3 mm; the strip was anchored by its other end to an aluminium block which was mounted, together with the transducer coil, on a rigid aluminum plate. Motion of the core relative to the coil of the transducer was determined by the mass of the core and its mounting, and by the elasticity of the phosphor bronze strip; it was therefore proportional to the acceleration of the whole device. The accelerometer was mounted on the piston of a modified Harvard Apparatus pump (model 607), the displacement of which was an approximately sinusoidal function of time. The accelerometer had a natural frequency of 200 cycles/sec and was underdamped; over the range of frequencies 0.5–10 cycles/sec, the output was 180° out of phase with displacement of the piston measured with a linear displacement transducer (Hewlett-Packard, 585Dt-2000), the core of which was rigidly attached to the piston.

The frequency response of a screen flowmeter in air was assessed by comparing ΔPs with the integral (Devices, model R 3030-3) of the output from the accelerometer; in sulfur hexafluoride, two screen flowmeters were coupled in series with a loudspeaker driven by a variable-frequency sine-wave generator. The two flowmeters were separated by a thin unstretched plastic sheet across which there was no pressure drop during periodic flow. This permitted one screen to be exposed to SF_6 and one to air; phase distortion was assessed by comparing ΔPs of the screen exposed to SF_6 with that of the screen exposed to air. Because there was no phase lag of flow with respect to ΔPs this same arrangement was used to assess the phase distortion of ΔPf with respect to flow; the Fleisch and screen flowmeters were separated by a lax plastic sheet and the phase lag of ΔPs with respect to ΔPf was measured with a storage oscilloscope, dual-trace amplifier, and calibrated time base (Tektronix, models 564, 3A72, and 2B67, respectively).

Amplitude Response

The amplitude of ΔPf was kept constant at each frequency and any phase lag between ΔPf and ΔPs was corrected by adding to ΔPf a signal proportional to acceleration[4]; the ratio of the amplitudes of the corrected and uncorrected signals was the ratio of the amplitude of periodic flow to the steady state flow rate at that ΔPf.

In these studies when SF_6 was substituted for air, Reynolds numbers (Re) at peak flow were maintained constant by reducing the peak flow rate in proportion to the decrease in kinematic viscosity. The loudspeaker was used in preference to the piston pump because with SF_6 that system was noisy and at low flow rates the signal-to-noise ratio was 5–15%; accurate measurements were therefore not possible with the mechanical pump.

RESULTS AND DISCUSSION

Steady-State Behavior

Capillary tube flowmeters. The V̇-P curve of each Fleisch flowmeter varied with the geometry of the tubing upstream from it, suggesting that ΔPf was a function of the distribution of the velocity of air, i.e., of the velocity profile, upstream from the flowmeter. The influence of some particular upstream geometries on the V̇-P curve of a no. 3 Fleisch flowmeter and the probable upstream velocity profiles associated with these geometries are shown in Fig. 1. The slopes of the V̇-P curves at the origins varied slightly being least in condition *D*. Within the nominal linear range of the flowmeter (0–6 liters/sec) the increase of ΔPf with increasing flow rate could be either disproportionately small (*A*) or disproportionately large (*B*). In *A*, where the flowmeter was preceded by a cone and a 50-cm-long pipe, the V̇-P curve had two approxi-

[2] In "flow" plethysmographs air is displaced into and out of the chamber through a resistive element in the wall; volume change is measured by integrating the pressure drop across the element and, in nonsteady-state conditions, correcting the integral for volume change due to compression of gas inside the chamber.

[3] Capillaries of Fleisch flowmeters are 32 mm long; ΔPf is usually measured as the pressure drop across the central 20 mm of the peripheral row of capillaries.

[4] Obtained by differentiating ΔPs with respect to time with an operational amplifier differentiator which had a time constant of 2.4 msec and a shunt capacitor of 0.001 μf across the resistor; its output was in phase with the output from the accelerometer over the range of frequencies 1–10 cycles/sec on air.

mately linear portions; at 6 liters/sec, ΔPf deviated from the extended initial portion of the curve by approximately 7%. In *B*, where the upstream geometry included another no. 3 flowmeter and a pipe of the same internal diameter as the flowmeter the V̇-P curve was linear from 0 to 2 liters/sec and continuously curvilinear at higher flows; at 6 liters/sec, ΔPf deviated from linearity by approximately 10%. In *C*, where the flowmeter was preceded by a converging cone, the V̇-P curve was linear from 0 to 3.2 liters/sec and curvilinear at higher flows; at 6 liters/sec, ΔPf deviated from linearity by approximately 7%. When the flowmeter was preceded by a large cross-sectional area such as the room ΔPf increased in proportion to flow to about 1.4 liters/sec, then increased proportionately less, and at about 3 liters/sec started increasing proportionately more than flow; at 6 liters/sec, ΔPf deviated by less than 3% from the extended initial portion of the curve. Small abrupt changes in the internal diameter or angulation of the tubing upstream from and adjacent to the flowmeter could change the V̇-P curve. When the upstream geometry remained constant and the downstream geometry was changed from a cone to a pipe of the same internal diameter as the flowmeter, the V̇-P curve did not change.

The influence of upstream geometry on the V̇-P characteristics of no. 2 and 4 Fleisch flowmeters was qualitatively similar to that described for the no. 3 flowmeter. The V̇-P curve of these flowmeters was linear over the widest range of flow rates when the immediate upstream geometry was a pipe of the same internal diameter as the flowmeter preceded by a cone with walls diverging in the direction of flow (Fig. 1*D*), i.e., some combination of the geometries illustrated in *A* and *B*, Fig. 1. The length of the pipe immediately upstream from the flowmeter and the linear V̇-P range achieved were: 2.5 cm and 0–2.4 liters/sec, 11 cm and 0–4.7 liters/sec, and 12 cm and 0–9.5 liters/sec for no. 2, 3, and 4 Fleisch flowmeters, respectively.

The total pressure drop across Fleisch flowmeters was nonlinear in flow from low flow rates; the relationship between flow and total ΔPf for a no. 3 flowmeter is shown in Fig. 2. At 6 liters/sec, total ΔPf deviated from the tangent to the origin of the V̇-P curve, i.e., from linearity, by 25%.

Screen flowmeters. ΔPs was nonlinear in flow from low flow rates and was influenced less by upstream geometry than ΔPf.

The V̇-P curve of five layers of 400-mesh screen covering a hole of 62 cm² in the wall of the 200-liter chamber and the curve of a single 12.9-cm² screen preceded by a 30-cm-long pipe with the same diameter as the screen are shown in Fig. 3 (top and bottom, respectively). ΔPs of the 12.9-cm² screen was the difference between the lateral pressures measured immediately adjacent to either side of the screen. At comparable flow rates, 10 liters/sec for the 62-cm² screen and 2 liters/sec for the 12.9-cm² screen, ΔPs deviated from linearity by approximately 11% in each. In the 12.9-cm² screen, ΔPs at a given flow was slightly less when the flowmeter was preceded by a cone than when preceded by the 30-cm-long pipe and at 2 liters/sec deviated from linearity by approximately 14%.

These results show how upstream geometry influences the V̇-P characteristics of flowmeters; in the following section we discuss the practical implications and interpretation of the results.

Implications. The degree of nonlinearity associated with any of the upstream geometries described here was small. Therefore, in estimating flow rate with Fleisch or 400-mesh screen flowmeters an incorrect assumption of linear V̇-P characteristics does not necessarily lead to notable inaccuracy. Estimates of flow rate may, however, be substantially inaccurate when the upstream geometry differs from that used when the flowmeter was calibrated, when measurements encompass a wide range of flow rates, or when the measured flow rates are outside the range for which the flowmeter was calibrated. For example, a Fleisch flowmeter used as in Fig. 1*A*, not calibrated at low flows, and assumed to be linear will overestimate flow rates near zero. Further, an assumption of linearity may obscure the V̇-P characteristics of the system being examined.

The practical implications of these results are: *1*) that flowmeters should be calibrated in situ, over the entire range of flows to be used; *2*) for measurements of flow in two directions the upstream and downstream geometries should be the same; *3*) changes of upstream geometry necessitate recalibration of the flowmeter; and *4*) the degree of nonlinearity in flow of the total ΔPf suggests that Fleisch flowmeters are not suitable for use as the resistive elements in "flow" plethysmographs.

Interpretation. Two mechanisms, acting separately or together, could explain why pressure drop at a given mean flow rate changed when upstream conditions changed. First, the distribution of flow among the parallel pathways of the flowmeter may be determined mainly by the distribution of velocity upstream. Second, local inertial forces associated with the geometry of the resistive elements may prevent, or delay, development of parabolic flow within the pathways of the flowmeter.

Evidence of the first mechanism was provided by a comparison of observed and predicted V̇-P curves for Fleisch flowmeters. The predicted V-P curve of a no. 3 flowmeter, calculated from the estimated average hydraulic radius of the capillaries[5] and assuming fully developed and evenly distributed flow, is shown by the interrupted line in Fig. 1*B*. The observed ΔPf was less than predicted suggesting that flow in the peripheral capillaries[3] was less than that which would have resulted from an even distribution of the total flow. The difference between the observed and predicted values was greatest where the velocity adjacent to the wall at a given mean flow rate would have been least, condition *A*, and was least where the velocity near the wall would have been greatest, condition *C*; with diverging flow (*A*) the velocity near the wall decreases and that near the center increases relative to fully developed flow: with converging flow (*C*) the effect is opposite.

That the distribution of flow among the resistive pathways is a function of the distribution of velocity upstream seems reasonable. The upstream velocity distribution tends to remain unchanged in the capillary network because of the inertia of the gas molecules along the axis of flow. If it did remain unchanged then the distribution of flow would be similar to the distribution of upstream velocity being greatest where axial velocity was greatest. The resistance of the pathways, however, modifies this tendency by producing a gradient of pressure across the section at their entrance: this gradient is a function of the upstream distribution of velocity and of the resistance of the flowmeter pathways. The effect is to produce a more uniform distribution of velocity at the entrance and therefore a more uniform distribution of flow. In summary, the distribution of flow among the pathways of a flowmeter depends upon the inertia of the fluid particles, and therefore on local velocity, and on the resistance of the flowmeter. A dimensional analysis of the V̇-P curves of the three sizes of Fleisch flowmeter, obtained with upstream geometries similar to that illustrated in Fig. 1*B*, supports this conclusion (Fig. 4). The dimensionless resistance of the peripheral capillaries is plotted against Re based on capillary diameter and the mean velocity. The dimensionless resistance was in each instance less than unity, i.e., less than predicted, and was least in the no. 4 flowmeter, i.e., in the flowmeter with the least resistance.

We interpret the change of ΔPs with change of upstream geometry as having the same basis as the similar results obtained with capillary tube flowmeters.

The shapes of the V̇-P curves are not readily interpreted. The

[5] Hydraulic radius (2 area/perimeter) was estimated with Poiseuille's law by counting the number of capillaries and measuring total ΔPf at low flow rates (<0.5 liter/sec) where pressure drop associated with entry effects would be small; it was 0.45 mm compared with 0.4 mm given by Fleisch.

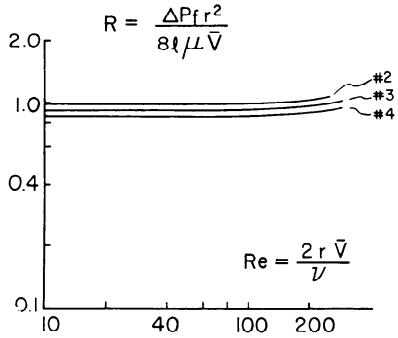

FIG. 4. Dimensionless resistance of no. 2, 3, and 4 Fleisch flowmeters vs. Re. Abbreviations: r = average hydraulic radius, l = length, μ = viscosity, $\bar{V}$ = mean velocity, ν = kinematic viscosity.

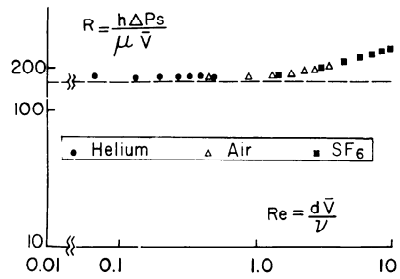

FIG. 5. Dimensionless resistance vs. Re of 12.9-cm² screen. Abbreviations: see text and legend of Fig. 4. Interrupted line is low Re intercept predicted from analysis of Keller.

alinearity of pressure in flow could reflect a redistribution of flow and/or a progressive change in the degree of development of flow within the parallel pathways as the mean flow rate changed. These mechanisms depend, respectively, on the upstream velocity distribution and on the ratio of inertial to viscous forces within the parallel pathways, i.e., on Re. In the capillaries of Fleisch flowmeters Re (in air) may be as high as 100–200 over a substantial part of the nominal linear flow range (Fig. 4) and will be proportionately higher for gas with a lower kinematic viscosity. These Re are sufficiently high for inertial forces to influence the development of flow in the capillaries. The greater alinearity in flow of the total ΔPf probably reflects the influence of the undeveloped nature of flow near the capillary entrance relative to that between the points at which ΔPf is usually measured. In these instances the V̇-P characteristics would become more linear if the length-to-diameter ratio of the capillaries was increased.

The degree to which a wire screen disturbs flow is a function of the Re pertinent to the wire diameter and hole size. In Fig. 5 the dimensionless resistance of a 400-mesh screen 12.9 cm² is plotted against Re based on the wire diameter;[6] an extended range of Re was examined by using gases of different kinematic viscosity.[7] The low Re intercept of dimensionless resistance was similar to that predicted from Keller's theoretical analysis[8] of viscous flow through a row of equal parallel cylinders (3), whereas the Re at which dimensionless resistance became dependent on Re (approximately 1.0) was similar to that predicted for inertial flow in the analysis of Tamada and Fujikawa (5). The similarity between our empirical results and those predicted by these analyses suggests that the alinearity of screen flowmeters relates chiefly to the influence of inertial forces on ΔPs. Tamada and Fujikawa showed that the range of linearity of pressure drop in flow increased as the ratio of the distance between the axis of the cylinders (h) and their diameters (d) decreased. Applying their results as an approximate guide to the behavior of screen flowmeters the smaller the ratio of hole size to wire diameter the greater will be the range of linear V̇-P characteristics for a given open area. The associated increase in resistance should also contribute to linearity by promoting a more even distribution of flow; practical limitations may be a disproportionate increase in resistance and an increased tendency to trap dust particles as the ratio h/d is decreased.

The steady-state V̇-P characteristics of flowmeters therefore represent a complex response of the entire system to the driving pressure; this relationship is analyzed in the APPENDIX.

Frequency Response

Capillary tube flowmeters. The effect of periodic flow on the amplitude and phase of flow with respect to ΔPf is shown in Fig. 6. The nondimensional quantity α is proportional to pipe radius and to the square root of the circular frequency ($\omega = 2\pi$ frequency, cycles/sec) divided by the kinematic viscosity; it expresses the proportionality between inertial and viscous forces during periodic flow. Flow amplitude measured at constant ΔPf is expressed as a ratio of the steady-state flow at that ΔPf; phase lag is the phase lag of flow with respect to ΔPf. The continuous lines are the amplitude and phase predicted for a long circular pipe with the same radius as the average hydraulic radius of the capillaries; the predictions are from the analysis of Womersley (6). For values of $\alpha < 0.8$, i.e., for the range of frequencies 0–10 cycles/sec on air, flow amplitude did not differ notably from steady-state flow but lagged ΔPf by 3–8.5°. For values of α greater than 1.0, i.e., for the range of frequencies 3–10 cycles/sec on SF_6, the flow amplitude at a given ΔPf departed markedly from the steady-state flow rate and the phase lag increased. ΔPf therefore reflects the magnitude but not the phase of periodic flow up to 10 cycles/sec on air; with gases of

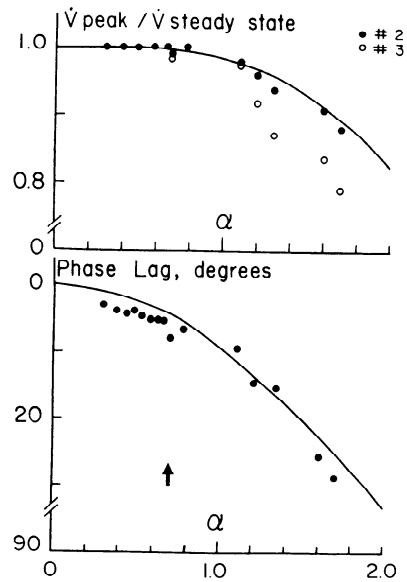

FIG. 6. Amplitude and phase of periodic flow of no. 2 (closed circles) and no. 3 (open circles) Fleisch flowmeters vs. α (defined in text). Arrow corresponds to a frequency of 10 cycles/sec in air.

[6] In calculating the Re and dimensionless resistance of 400-mesh screen, $\bar{V}$ was the mean velocity pertinent to flow upstream from the flowmeter, i.e., the "undisturbed velocity."

[7] In these studies a bag-in-box technique was used to estimate flow rate: the test gas was withdrawn from a balloon through the screen flowmeter; the balloon was sealed in a box vented to the atmosphere through a no. 4 Fleisch flowmeter.

[8] Modified to the case of a mesh with square openings by multiplying the pressure drop by $4\,h/h - d$; h is the distance between wire axes and d is their diameter. This factor was derived using the hydraulic radius to define the ratio of pressure drop for fully developed laminar flow through a mesh to that through a row of parallel cylinders.

low kinematic viscosity ΔPf may vary substantially in both amplitude and phase from true flow.

The behavior of capillary tube flowmeters during periodic flow is due to the inertia of the gas; because of the momentum of the gas molecules, flow tends to continue in the original direction when the driving pressure is reversed. Flow therefore lags the driving pressure; as frequency increases and inertial forces increase, more and more of the available driving pressure will be spent in accelerating and decelerating the gas. Flow will progressively lag pressure and, at a given driving pressure, the amount of flow generated will become less and less.

The implications of these results to estimating oscillatory flow rates are that up to α's of 1.3 the steady-state $\dot{V}$-P calibration can be applied with accuracy; for higher α's, and where accurate measurements of the phase of flow are required, calibration of phase and amplitude with respect to the range of α's to be used is necessary.

The frequency response of Fleisch flowmeters can be improved by adding to ΔPf, in the appropriate sign, a signal proportional to acceleration. In practice ΔPf and a standard signal proportional to flow are displayed X and Y on an oscilloscope; at a fixed frequency, a signal proportional to acceleration is added to ΔPf until the summed signal, judged by its relationship to the standard signal, has the phase appropriate for flow. Because inertial forces are proportional to acceleration a correction made at one frequency should be appropriate to all other frequencies; in practice we have found this to be the case. The signal proportional to acceleration may be obtained from an accelerometer attached to the pump or by differentiating flow with respect to time.[9]

Screen flowmeters. There was no phase lag between ΔPs and flow at frequencies up to 10 cycles/sec on both air and SF_6. This frequency response is appropriate to the small size of the screen openings; the hydraulic radius was approximately 18×10^{-4} cm which means that the highest α was about 0.09.

We have previously observed (Finucane, Green, and Mead, unpublished data) that nonlinear $\dot{V}$-P relationships (e.g., those of short tubes and of orifices) tend to become progressively more linear, while their slopes at the origin tend to decrease, as α is increased or as peak amplitude is increased at a given α. A similar effect of frequency on the $\dot{V}$-P curve of a 12.9-cm² flowmeter was noted. Although the effect was small at flow amplitudes <2.0 liters/sec, at larger amplitudes of periodic flow the slope at the origin was sufficiently different from the slope during steady-state flow for flow rate to be substantially overestimated.

This study shows that the $\dot{V}$-P characteristics of capillary tube and 400-mesh screen flowmeters are determined by the physical properties of the flowmeter itself and by the geometry of the system in which it is incorporated. It leads to the conclusion that in low-resistance flowmeters the distribution of flow is not independent of the system in which the flowmeter is incorporated and that accurate measurements of flow rate require information of $\dot{V}$-P characteristics over the full range of flow rates to be estimated, obtained under the circumstances in which it is intended to use the flowmeter.

APPENDIX

Distribution of Flow Upstream From a Flow-Resistive Element With Uniform Parallel Pathways

The distribution of flow through the uniformly sized openings of a fine mesh screen or bundle of capillary tubes inserted in a pipe is generally more uniform than the distribution of flow across the section of the pipe far upstream from either sort of resistive element. The presence of the resistive element causes a radial gradient of the static pressure to be established immediately upstream; this gradient alters the distribution of velocity, acting to distribute the flow more evenly among the pathways of the resistive element.

[9] ΔPf, differentiated as described in footnote 4, except that the shunt capacitor has a value of 0.01 μf, is in phase with acceleration over the range of frequencies 1–10 cycles/sec on air.

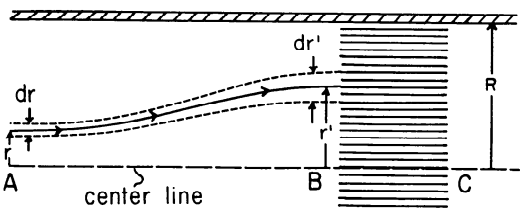

FIG. 7. Resistive element (B — C) and typical fluid element flowing along a streamline from station A to station B.

Here we present a mathematical analysis which shows how the balance between the viscous forces exerted by the resistive element and the inertial forces arising in the fluid determines the distribution of flow in the pathways of the element. We use this analysis to describe the departures to be expected from a uniform distribution of flow for a particular upstream velocity profile and various values of resistance of the element. The analysis is for the case of laminar flow and therefore may not be accurate in quantitative detail for the cases of turbulent flow that will usually be encountered in flowmeters.

Analysis. Upstream from the resistive element (see Fig. 7) we assume that the flow is axisymmetric and laminar and behaves inviscidly: that pressure forces are in balance with inertial forces. Far upstream, at station A, we assume that the static pressure, P_A, is constant, independent of the radial coordinate from the pipe center line and that the velocity distribution has the form, $V_A(r)$. In Fig. 7 we note that fluid in a stream tube which passes station A at a radial coordinate, r, and with a radial increment, dr, flows past station B at a radial coordinate, r', and with a radial increment, dr'. Continuity of mass for an incompressible fluid requires that:

$$V_A(r)\, r dr = V_B(r') r' dr' \qquad (A\text{-}1)$$

We anticipate that both the fluid velocity and the static pressure at B will be a function of radial coordinate. Because the flow behaves inviscidly in the upstream section, Bernouli's principle requires that along a streamline from A to B we have

$$P_A + \rho V_A^2(r)/2 = P_B(r') + \rho V_B^2(r')/2 \qquad (A\text{-}2)$$

where ρ is the density of the fluid. We assume that the flow within each pathway of the resistive element is dominated by viscous forces. With the further assumption that the pressure downstream of the resistive element, P_c, is constant we may write for a fluid element entering the resistance at radial coordinate, r':

$$P_B(r') - P_c = k V_B(r') \qquad (A\text{-}3)$$

where $k = 8\epsilon L\mu/a^2$, pathway resistance; μ = viscosity of fluid; L = length of pathway; a = hydraulic radius of pathway; and ϵ = proportion of open cross section.

Combining *equations A-2* and *A-3* we have

$$\rho V_B^2(r')/2 + k V_B(r') = \rho V_A^2(r)/2 + P_A - P_c$$

Solving for $V_B(r')$ and discarding the negative root we obtain

$$V_B(r') = k/\rho + \{(k/\rho)^2 + V_A^2(r) + 2(P_A - P_c)/\rho\}^{1/2} \qquad (A\text{-}4)$$

Rearrangement of *equation A-1* and integration radially from the pipe axis to a typical streamline yields

$$\int_0^{r'} r' dr' = \int_0^{r'} \{V_A(r)/V_B(r')\} r dr \qquad (A\text{-}5)$$

Let $f(r) = V_A(r)/\bar{V}$, where $\bar{V}$ is mean velocity through the pipe, and substitute *equation A-4* into *equation A-5*,

$$(r')^2/2 = \int_0^r \{f(r)/\{-k/\rho\bar{V} + (k/\rho\bar{V})^2 + f^2(r) + 2(P_A - P_c)/\rho\bar{V}^2\}^{1/2}\} r dr \qquad (A\text{-}6)$$

$$= \frac{1}{F}\int_0^r \{f(r)/\{-1 + (1 + f^2/F^2 + \bar{P}/F^2)\}^{1/2}\} r dr$$

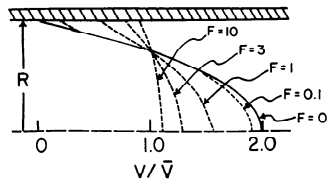

FIG. 8. Relative distribution of velocity, $V/\bar{V}$, from center line to wall at station B as a function of friction parameter F.

TABLE 1. *Relationship between dimensionless parameters F and $\tilde{P}$ and relative velocity on center line and on pipe wall*

F	0.03	0.1	0.3	1.0	3.0	10	30	100
$\tilde{P}$	0.0095	0.0594	0.288	1.41	5.19	19.1	59.1	198.6
$V_B(O)/\bar{V}$	1.973	1.917	1.792	1.532	1.265	1.093	1.038	1.008
$V_B(R)/\bar{V}$	0.072	0.163	0.314	0.552	0.767	0.912	0.964	0.998

where $\tilde{P} = 2(P_A - P_c)/\rho\bar{V}^2$, a dimensionless pressure parameter, and $F = k/\rho\bar{V}$ a dimensionless parameter denoting the importance of frictional resistance compared to flow inertia.

Solution for upstream parabolic velocity profile. With an upstream velocity profile which is parabolic,

$$f(r) = 2(1 - (r/R)^2) \qquad (A\text{-}7)$$

equation A-6 can be integrated out to the pipe wall to yield a transcendental equation relating average velocity to overall pressure drop.

$$1 = F/2[(1 + 4/F^2 + \tilde{P}/F^2)^{1/2} - (1 + \tilde{P}/F^2)^{1/2} + \log((1 + 4/F^2 + \tilde{P}/F^2)^{1/2} - 1) - \log((1 + \tilde{P}/F^2)^{1/2} - 1)] \qquad (A\text{-}8)$$

Values of $\tilde{P}$ vs. F obtained from the solution of this equation are presented in Table 1.

The velocity profile $V_B(r')$ is found from *equation A-4* after getting r' as a function of r by integrating *equation A-6* with variable end point,

$$(r')^2/2 = -F[m(r) - m(O) + \log(m(r) - 1)/(m(O) - 1)]$$

where $m^2(r) = 1 + (f(r)/F)^2 + \tilde{P}/F^2$. In the same notation, *equation A-4* becomes

$$V_B(r')/\bar{V} = F(-1 + m(r))$$

which is the relative velocity plotted in Fig. 8 as a function of the radial coordinate at station B. Values of relative velocity on the center line and on the pipe wall are also given at station B in Table 1.

In noting the progressive flattening of velocity profile as the friction parameter, F, is increased, it may be seen that all profiles assume their average value at about the same value of radial coordinate ($r/R = 0.7$), an observation that may have implication in design of flowmeters. The failure of velocity profiles to go to zero on the pipe walls as expected for real fluids is also noted. This results from the neglect of viscous forces in the upstream flow. This is a valid assumption for the description of flow in a pipe of uniform cross section because boundary-layer theory would show a sharp transition of velocity to zero very near the wall, with velocities in the bulk of the flow being accurately predicted.

We thank Dr. Jere Mead for his helpful assistance and evaluation of these studies and for reviewing an earlier version of this manuscript.

These studies were supported by National Institutes of Health Grant HE-13843 and by the National Air Pollution Control Administration, Consumer Protection and Environmental Health Service, Public Health Service under Grant APO1010-01.

The empirical description of flowmeter behavior was made by K. E. Finucane, an Overseas Fellow of the Royal Australasian College of Physicians, and the analytical description by B. A. Egan and S. V. Dawson.

Present address of K. E. Finucane: Dept. of Lung Physiology, Sir Charles Gairdner Hospital, Verdun St., Shenton Park, Western Australia 6008.

Received for publication 25 March 1971.

REFERENCES

1. FLEISCH, A. Pneumotachograph: apparatus for recording respiratory flow. *Arch. Ges. Physiol.* 209: 713–722, 1925.
2. FRY, D. L., R. E. HYATT, C. B. MCCALL, AND A. J. MALLOS. Evaluation of three types of respiratory flowmeters. *J. Appl. Physiol.* 10: 210–214, 1957.
3. KELLER, J. B. Viscous flow through a grating or lattice of cylinders. *J. Fluid Mech.* 18: 94–96, 1963.
4. SILVERMAN, L., AND J. L. WHITTENBERGER. Clinical pneumotachograph. In: *Methods in Medical Research.* Chicago, Ill.: Year Book, 1954, vol. 2, p. 104–112.
5. TAMADA, K., AND H. FUJIKAWA. The steady two dimensional flow of viscous fluid at low Reynolds numbers passing through an infinite row of equal parallel cylinders. *Quart. J. Mech. Appl. Math.* 10: 425–432, 1957.
6. WOMERSLEY, J. F. Method for the calculation of velocity, rate of flow and viscous drag in arteries when the pressure gradient is known. *J. Physiol., London* 127: 553–563, 1955.